

# Hyperbolic chaos in the phase dynamics of a Q-switched oscillator with delayed nonlinear feedbacks

S. P. KUZNETSOV<sup>1,2</sup> and A. PIKOVSKY<sup>2(a)</sup>

<sup>1</sup> *Kotel'nikov Institute of Radio Engineering and Electronics of RAS, Saratov Branch  
Zelenaya 38, Saratov, 410019, Russian Federation*

<sup>2</sup> *Department of Physics and Astronomy, Potsdam University - 14476 Potsdam-Golm, Germany, EU*

received 12 June 2008; accepted in final form 29 August 2008

published online 26 September 2008

PACS 05.45.Ac – Low-dimensional chaos

PACS 42.65.Sf – Dynamics of nonlinear optical systems; optical instabilities, optical chaos and complexity, and optical spatio-temporal dynamics

**Abstract** – We propose a device based on a *Q*-switched self-sustained oscillator with two nonlinear delayed feedback loops. Due to the appropriate phase transformation of the signal that influences the generation of each successive pulse, the phase difference between the two neighboring pulses evolves according to the Bernoulli doubling map. It corresponds to a hyperbolic chaotic attractor yielding a robust, structurally stable chaos. We discuss possible experimental implementations of the scheme.

Copyright © EPLA, 2008

Although deterministic chaos is ubiquitous in natural and technical systems, its mathematical description is far from being complete. In a mathematical theory of dynamical systems one introduces a class of uniformly hyperbolic chaotic attractors [1–3]. In such attractors all orbits are of saddle type, with stable and unstable manifolds of equal dimension all over the attractor, and no tangencies between the manifolds occur: their intersections can be only transversal. The dynamics on such attractors possesses strong chaotic properties and allows a precise mathematical analysis. For about 40 years of existence of the corresponding mathematical theory, it was commonly believed that the hyperbolic chaotic attractors are not relevant for real-world systems with complex dynamics. In textbooks and tutorials, the traditional examples of such attractors are represented by rather artificial constructions, the Plykin attractor [4] and the Smale-Williams solenoid [1].

Recently, several examples of realistic systems with attractors of the Smale-Williams type have been suggested [5–8]. A general principle behind the construction of these models is a manipulation of the phases of oscillations in the course of the excitation transfer between two (or more) alternating self-oscillatory systems.

In this letter we exploit the same main idea to construct a chaotic system on a base of a single active element.

We consider a *Q*-switched self-sustained oscillator demonstrating periodically alternating activity, interrupted with stages of silence. The oscillator is supplemented with two additional nonlinear delayed feedback loops. Due to this feedback, when the oscillator enters a new active stage, its phase is determined by the phases from two previous activity stages through a chaotic map. The presence of the delay complicates the mathematical nature of the model (formally, the phase space of the system becomes infinite dimensional), but in a physical implementation the delays can be arranged rather easily.

As we hope, the proposed scheme is mostly appropriate for a realization with lasers. There the *Q*-switching—the method of obtaining pulses from lasers by modulating the intracavity losses—is a widespread tool for designing of a pulsed laser generation (see, *e.g.*, [9], Chapt. 26). Our setup below in fig. 1 corresponds to the so-called active *Q*-switch, where the modulation is achieved by applying an external signal via, typically, an acousto-optic or an electro-optic modulator. Here one can explicitly control the periodicity of the pulse train, contrary to the case of a passive *Q*-switch, where pulsation appears due to an instability of the continuous generation because, *e.g.*, of a saturable absorber. Nonlinear delayed feedback loops are also a common scheme in laser experiments [10], where very efficient methods for the second and the third harmonic generation have been developed [11–14]. However, in the presentation below we do not follow a

<sup>(a)</sup> E-mail: pikovsky@uni-postdam.de

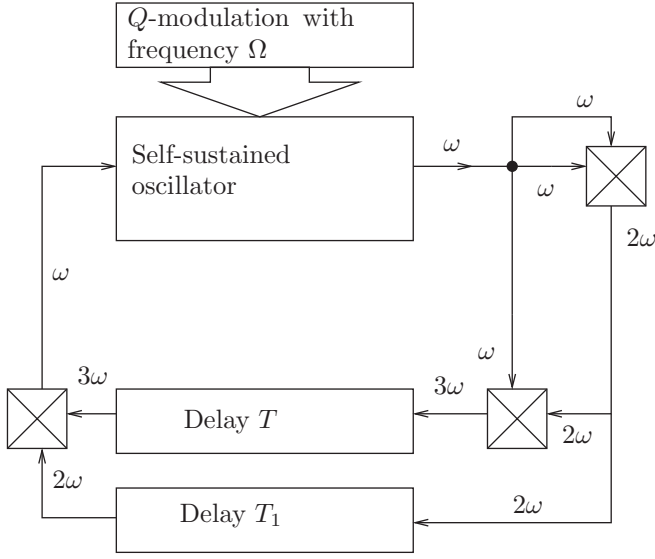


Fig. 1: Block diagram of the system. Crossed boxes are nonlinear elements —quadratic multipliers. The feedback loop includes two delay units with times  $T$  and  $T_1$ . A separate block is a modulator with frequency  $\Omega$  controlling the periodic Q-switch of the self-oscillator, the main element of the device.

description for a particular type of laser, rather we deal with a generalized mathematical model for a self-sustained oscillator, valid for a wide class of systems. For example, the proposed scheme is relevant also for experiments with electronic circuits, because all essential features (a periodic modulation of losses, a nonlinear transformation of a quasiharmonic signal, a delay) can be easily realized electronically.

The block diagram of the system is shown in fig. 1. It contains the main active element, a self-sustained oscillator with the operating frequency  $\omega$ . Because of a slow external modulation of the activity/losses with frequency  $\Omega \ll \omega$ , the oscillator becomes active periodically with period  $\tau = 2\pi/\Omega$ , and the stages of activity are interrupted with intervals of silence (see fig. 2(a) below). We denote successive pulses of oscillation with indices  $\dots n-1, n, n+1 \dots$ . If there were no additional feedback loops (depicted in the lower part of the block diagram), the phase of each new pulse were arbitrary, because each pulse grows from very small amplitudes on which the field is essentially noisy and the phase is not defined.

Let us consider how this sequence of pulses with undetermined phases is modified by the delayed feedback loops. Introducing the amplitude  $f_n$  and the phase  $\varphi_n$  of the  $n$ -th pulse, we can represent the oscillatory process as  $x(t) = \sum_n f_n(t) \cos(\omega t + \varphi_n)$ . The time constants of the delay loops,  $T$  and  $T_1$  are chosen in such a way, that the  $(n-1)$ -th pulse delayed by time  $T_1$  and the  $n$ -th pulse delayed by time  $T$  overlap during the time interval, when the intensity of the  $(n+1)$ -th pulse starts to grow. (This means that the optimal value for  $T$  is slightly less than  $\tau$ , and the optimal value for  $T_1$  is  $T + \tau$ ; in our numerics

below we use  $\tau = 2\pi$ ,  $T = 5$  and  $T_1 = 11$ .) In the input of the delay line  $T$  we send the third harmonics of the process  $x(t)$ , this is obtained by means of two multipliers with quadratic nonlinearity. Thus, at the output of the delay line  $T$  we have a process  $\propto f_n^3 \cos(3\omega t + 3\varphi_n + \text{const})$ . In the input of the delay line  $T_1$  we send the second harmonics of the process  $x(t)$ . Thus, at the output of this delay line we have a process  $\propto f_n^2 \cos(2\omega t + 2\varphi_n + \text{const})$ . Note that all other harmonics possible at the outputs of the delay lines are supposed to be filtered out. These two processes from the outputs of the delay lines are mixed in the quadratic multiplier, and the resulting component at frequency  $\omega$  is proportional to  $f_n^3 f_{n-1}^2 \cos(\omega t + 3\varphi_n - 2\varphi_{n-1} + \text{const})$ . This harmonic component resonantly forces the self-sustained oscillator at the beginning of the activity stage  $(n+1)$  and serves as a “germ” for the excitation of the oscillator. It means that the pulse  $(n+1)$  will adopt the phase of the forcing according to the relation

$$\varphi_{n+1} = 3\varphi_n - 2\varphi_{n-1} + \text{const}. \quad (1)$$

This discrete-time evolution of phases, from one pulse to another, can be interpreted in terms of the one-dimensional dynamics, if we introduce the phase difference between the successive pulses

$$\vartheta_n = \varphi_n - \varphi_{n-1}. \quad (2)$$

As follows from (1), this new variable will behave in accordance with the expanding map of a circle, the so-called Bernoulli doubling map [2,15]:

$$\vartheta_{n+1} = 2\vartheta_n + \text{const} \pmod{2\pi}. \quad (3)$$

(The constant in the equation, which depends on delay times and details of manipulation with signals in the feedback loops is of no principal significance because it can be removed from the equation by an appropriate selection of the offset for the variable  $\vartheta$ .)

After the qualitative explanation of the phase transformation, let us turn to a consideration of the delay differential equation corresponding to the block diagram of fig. 1. Representing the oscillatory process  $x(t)$  by means of the slowly varying complex amplitude  $x = \text{Re}[a(t)e^{i\omega t}]$ , we can write for this amplitude

$$\frac{da}{dt} = (\gamma_0 + \gamma_1 \cos \Omega t - |a|^2)a + \varepsilon[a(t-T)]^3[a^*(t-T_1)]^2. \quad (4)$$

The oscillator is assumed to be of the Stuart-Landau type, the modulation of the parameter responsible for its excitation follows the expression  $\Gamma(t) = \gamma_0 + \gamma_1 \cos \Omega t$ . The stages of activity correspond to  $\Gamma(t) > 0$ , and those of silence to  $\Gamma(t) < 0$ . The structure of the retarded terms in the right-hand part is selected in accordance with the signal transformations in the feedback loops, as described in our qualitative considerations above. From all possible terms appearing when the signal of the third harmonic

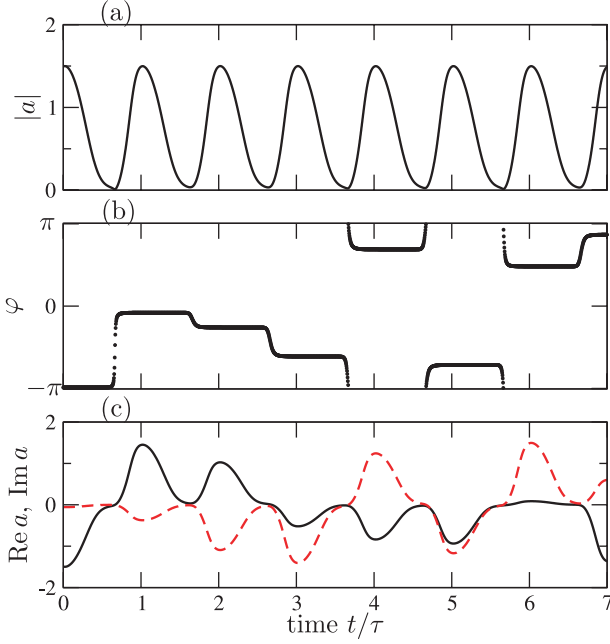


Fig. 2: (Color online) Modulus of the amplitude (a), the phase  $\varphi = \arg(a)$  of the oscillator (b), and real and imaginary parts of the complex amplitude (c) *vs.* time, obtained from a numerical solution of eq. (4) at  $\Omega = 1$ ,  $\gamma_0 = 0.2$ ,  $\gamma_1 = 2$ ,  $\varepsilon = 0.1$ ,  $T = 5$ , and  $T_1 = 11$ . Simulations have been checked by using different numerical methods, in particular a predictor-corrector scheme with fixed time step  $\Delta t = 0.00125$ .

with delay time  $T$ , and the signal of the second harmonic with delay time  $T_1$  are multiplied, we chose only the resonant term at frequency  $\omega$ . It is proportional to  $[a(t - T)]^3[a^*(t - T_1)]^2$ , where  $a^*$  denotes the complex conjugate. The overall performance of the three quadratic multipliers and the delay lines is summarized in a single complex parameter, the feedback strength  $\varepsilon$ . Non-resonant terms practically do not affect the oscillator and are therefore neglected.

Figures 2 and 3 show some results of numerical simulation of the system dynamics at a particular set of the dimensionless parameters  $\Omega = 1$ ,  $\gamma_0 = 0.2$ ,  $\gamma_1 = 2$ ,  $\varepsilon = 0.1$ ,  $T = 5$ , and  $T_1 = 11$ . From fig. 2 one can conclude that the amplitudes of the pulses are nearly equal (panel (a)), while the phases are different from pulse to pulse (within a pulse the phase is nearly constant, panel (b)). In fig. 3 we present a stroboscopic mapping of the phase difference  $\vartheta_n$ , it nearly perfectly corresponds to the theoretical prediction (3). In fig. 4 we illustrate similarity of the attractor in eq. (4) to the Smale-Williams solenoid. For this, we chose a special stroboscopic observation at a particular phase of  $Q$ -switching, because at other phases of this cycle the fractal transverse structure is hardly visible.

To characterize further the chaotic dynamics we have calculated the 7 largest Lyapunov exponents in dependence on the feedback strength  $\varepsilon$  for  $\gamma_0 = 0.2$  and  $\gamma_1 = 2$ , see fig. 5. One can see that there is no chaos for  $\varepsilon < 0.05$ . For  $\varepsilon > 0.065$  we observe a hyperbolic chaos as described

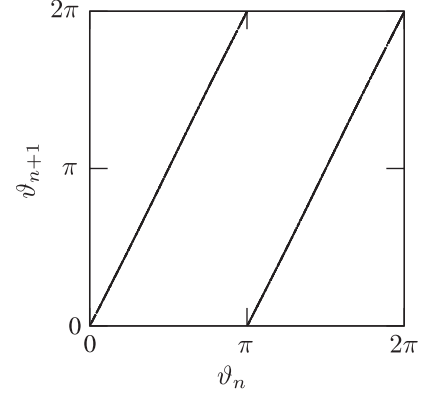


Fig. 3: Iteration diagrams for the phase differences obtained from numerical simulation of the dynamics of eqs. (4), the parameters are the same as in fig. 2. The phases  $\varphi_n$  are taken stroboscopically at times  $\tau, 2\tau, \dots$ , from them the phase differences according to eq. (2) are calculated. Observe a good agreement with expression (3): the sets of points look like straight lines.

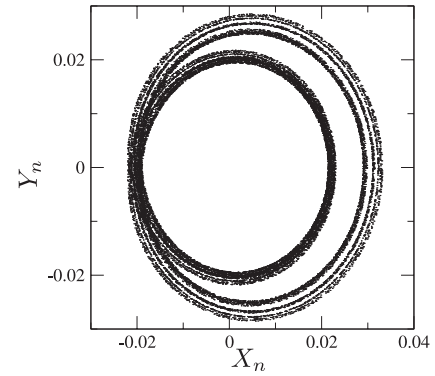


Fig. 4: A stroboscopic portrait illustrating a similarity of the attractor in eq. (4) to the Smale-Williams solenoid. The pictures are drawn in projection on the plane  $(X_n, Y_n)$ , where  $X_n + iY_n = a(n\tau + \tau_0)a^*((n-1)\tau + \tau_0)$ ,  $\tau = 2\pi/\Omega$ ,  $\tau_0 = 8\tau/11$ . The parameters are the same as in fig. 2.

above; it has one positive Lyapunov exponent. Its value corresponds to multiplications of a small state perturbation approximately by factor of 2 over a period of the  $Q$ -modulation  $\tau$ , in a good agreement with what one expects from eq. (3). Additionally, the system possesses a zero Lyapunov exponent corresponding to the invariance of eq. (4) in respect to the phase shift. All other exponents are negative. The Lyapunov dimension of the attractor in this parameter range is between 1.5 and 2.5. In fig. 5 one can also see a transitional region  $0.05 < \varepsilon < 0.065$ , where the largest Lyapunov exponent is positive but less than the value following from eq. (3). Here, presumably, a non-hyperbolic chaos occurs. As the problem of the transition to hyperbolic chaos under parameter variations is yet unresolved neither in mathematical nor in physical literature, we postpone a study of the transitional region to the future.

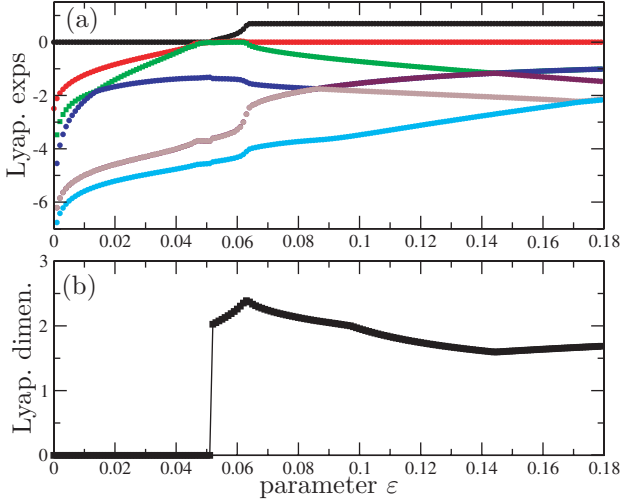


Fig. 5: (Color online) Panel (a): Seven largest Lyapunov exponents (normalized by period  $\tau$ , filled circles of different colors) in eq. (4) as functions of the feedback strength  $\varepsilon$  (which is assumed to be real). The Lyapunov dimension (panel (b)) is calculated by neglecting the zero Lyapunov exponent corresponding to the phase invariance.

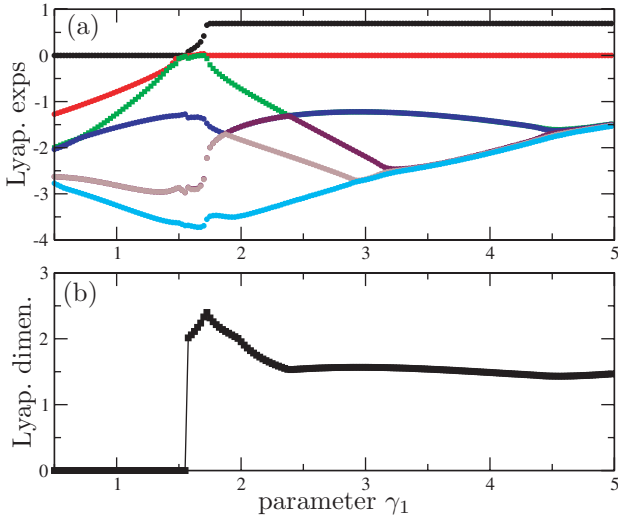


Fig. 6: (Color online) Panel (a): Seven largest Lyapunov exponents (normalized by period  $\tau$ , filled circles of different colors) in eq. (4) as functions of the modulation level  $\gamma_1$ . The Lyapunov dimension (panel (b)) is calculated by neglecting the zero Lyapunov exponent corresponding to the phase invariance.

In fig. 6 we perform a similar analysis for the dependence on the modulation level  $\gamma_1$ , for fixed values  $\varepsilon = 0.1$  and  $\gamma_0 = 0.2$ . The behavior is qualitatively similar to that of fig. 5: there is a large range of this parameter  $1.8 < \gamma_1 < 5$  where the hyperbolic chaos is observed.

At all values of the parameters presented in figs. 5, 6 we observed a single attractor and no multistability. While generally a multistability may appear in systems with delay, in our setup the attracting domain in the phase space is largely determined by the non-delayed

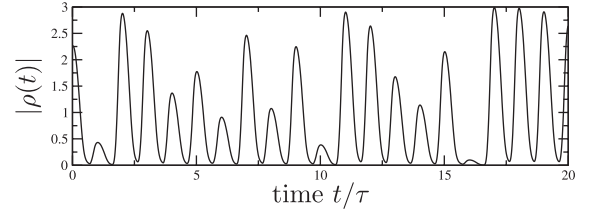


Fig. 7: The observable  $|\rho(t)| = |a(t) + a(t - \tau)|$  vs. time for the same parameters as in fig. 2. Contrary to fig. 2(a), this observable demonstrates chaotically varying pulse amplitudes.

dynamics, which is simply a response of a self-sustained oscillator to the modulation of losses and shows therefore no multistability. The delayed feedback is relatively weak as it serves only for the phase transfer, therefore it does not lead to multistability as well. One can expect multistability to appear only for rather large values of the feedback parameter  $\varepsilon$ .

We would like now to discuss, how the hyperbolic chaos can be detected in experiments. As we have laser experiments in mind, a direct registration of the phases seems hardly possible. However, a proper observable may be obtained by looking on the interference between two successive pulses. Indeed, the sum of the pulse fields

$$\rho(t) = a(t) + a(t - \tau) \quad (5)$$

demonstrates a strong irregular variability of intensity (fig. 7). Assuming that the amplitude  $A$  of the field  $a(t)$  is periodic and only the phase changes, we can write  $\rho(t) = A(t)(e^{i\varphi(t)} + e^{i\varphi(t-\tau)})$  and for the modulus we obtain a strong dependence on the phase difference

$$\begin{aligned} |\rho(t)| &= |A| \cdot |1 + e^{i(\varphi(t) - \varphi(t-\tau))}| \\ &= |A| \sqrt{2(1 + \cos(\varphi(t) - \varphi(t-\tau)))}. \end{aligned}$$

The dynamics of the observable  $\rho$  can be also characterized via a stroboscopic map. Because  $|\rho_n|^2 = 2|A_n|^2(1 + \cos \vartheta_n)$  and  $A_n \approx \text{const}$ , such a map is just a nonlinearly transformed Bernoulli doubling map (3). The most simplest form this map has if the constant in (3) vanishes, then the stroboscopic map for  $|\rho_n|^2$  is the logistic map in the regime of full chaos, see fig. 8.

In conclusion, we have suggested a simple feedback scheme that leads to a hyperbolic chaotic dynamics in a  $Q$ -switched self-sustained oscillator. We have considered the case of active  $Q$ -switching, but the same mechanism will work for a passive  $Q$ -switching as well, although it will require more careful selection of the delay times.

In comparison with schemes proposed in our previous works [5–8,16], the present one has several advantages from the point of view of a possible experimental realization. First, the use of a single oscillatory element obviously simplifies the device in comparison to those with two or more active elements (one does not have a problem of adjusting the parameters etc.). Second, in this scheme we exploit a *resonant* transmission of the excitation from the

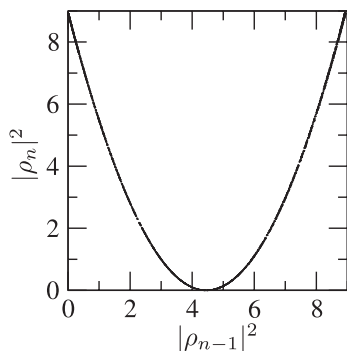


Fig. 8: The stroboscopic map of the variable  $|\rho_n|^2$  for the same parameters as in fig. 2.

previous activity stages to the next one, which appears to be possible because of the use of two delays and of the signal transformations involving the second and the third harmonics. As the resonance condition is automatically satisfied in this scheme, there is no problem with adjusting the frequencies; moreover, the feedback can be relatively small. The resonant mode of operation allows us to describe the system in terms of slowly varying complex amplitudes, so that the equations do not contain the basic frequency at all. This makes the model relevant for a wide range of oscillators—from very fast (lasers) to extremely slow (chemical reactions) ones. The robust hyperbolic chaos manifests itself in the dynamics of the phase variable, which is hardly observable in optics, but using the “interference” technique it is possible to reveal it via a chaotically varying intensity. As the hyperbolic strange attractors are structurally stable objects, the scheme may have advantages for applications in all cases where a robust low-dimensional chaos is needed, *e.g.* in chaotic communication. This property of a hyperbolic chaos distinguishes it from a chaos that typical smooth dynamical systems, like *e.g.* Rössler system, demonstrate. Indeed, in the Rössler-type system as well as in general smooth unimodal maps the chaotic regions are intermingled in parameter space with periodic windows. The set of parameters for which chaos is observed is typically a fat fractal set with holes everywhere (although in numerical and physical experiments small periodic windows are practically unobservable). Although one can construct families of chaotic smooth unimodal maps like in [17], this does not mean their robustness with respect to *generic*

perturbations. Contrary to these systems, the hyperbolic chaotic attractor constructed in this letter is structurally stable to generic perturbations and exists in a rather large range of parameters. Moreover, as the symbolic dynamical description of the Bernoulli doubling map (3) is robust, one can reliably employ it in communication schemes.

\*\*\*

We thank M. OSTERMEYER for useful discussions. The research was supported, in part, by the DFG grant 436-RUS-113/949. SPK acknowledges partial support from RFBR, grant No. 06-02-16773.

## REFERENCES

- [1] SMALE S., *Bull. Am. Math. Soc.*, **13** (1967) 747.
- [2] KATOK A. and HASSELBLATT B., *Introduction to the Modern Theory of Dynamical Systems* (Cambridge University Press) 1995.
- [3] BRIN M. and STUCK G. J., *Introduction to Dynamical Systems* (Cambridge University Press, Cambridge) 2002.
- [4] PLYKIN R., *Math. USSR Sb.*, **23** (1974) 233.
- [5] KUZNETSOV S. P., *Phys. Rev. Lett.*, **95** (2005) 144101.
- [6] KUZNETSOV S. P. and SELEZNEV E. P., *J. Exp. Theor. Phys.*, **102** (2006) 355.
- [7] KUZNETSOV S. P. and SATAEV I. R., *Phys. Lett. A*, **365** (2007) 97.
- [8] KUZNETSOV S. and PIKOVSKY A., *Physica D*, **232** (2007) 87.
- [9] SIEGMAN A. E., *Lasers* (University Science Books, Mill Valley, Cal.) 1986.
- [10] BOYD R. W., *Nonlinear Optics* (Academic Press, San Diego) 2003.
- [11] SÜDMEYER T., IMAI Y., MASUDA H., EGUCHI N., SAITO M. and KUBOTA S., *Opt. Express*, **16** (2008) 1546.
- [12] SEKA W., JACOBS S. D., RIZZO J. E., BONI R. and CRAXTON R. S., *Opt. Commun.*, **34** (1980) 469.
- [13] EIMERL D., AUERBACH J. M., BARKER C. E., MILAM D. and MILONNI P. W., *Opt. Lett.*, **22** (1997) 1208.
- [14] YUAN P., QIAN L., ZHENG W., LUO H., ZHU H. and FAN D., *J. Opt. A: Pure Appl. Opt.*, **9** (2007) 1082.
- [15] OTT E., *Chaos in Dynamical Systems* (Cambridge University Press, Cambridge) 1992.
- [16] JALNINE A. Y. and KUZNETSOV S. P., *Phys. Rev. E*, **77** (2008) 036220.
- [17] ANDRECUT M. and ALI M. K., *Phys. Rev. E*, **64** (2001) 025203.